

APPARATUS AND DEMONSTRATION NOTES

The downloaded PDF for any Note in this section contains all the Notes in this section.

Frank L. H. Wolfs, *Editor*

Department of Physics and Astronomy, University of Rochester, Rochester, New York 14627

This department welcomes brief communications reporting new demonstrations, laboratory equipment, techniques, or materials of interest to teachers of physics. Notes on new applications of older apparatus, measurements supplementing data supplied by manufacturers, information which, while not new, is not generally known, procurement information, and news about apparatus under development may be suitable for publication in this section. Neither the *American Journal of Physics* nor the Editors assume responsibility for the correctness of the information presented.

Manuscripts should be submitted using the web-based system that can be accessed via the *American Journal of Physics* home page, <http://ajp.dickinson.edu> and will be forwarded to the ADN editor for consideration.

Visible optical beats at the hertz level

Mickey McDonald^{a)}

Department of Physics, Columbia University, New York, New York 10027

Jiyoun Ha

Tenaflly High School, Tenaflly, New Jersey 07670

Bart H. McGuyer and Tanya Zelevinsky

Department of Physics, Columbia University, New York, New York 10027

(Received 1 October 2013; accepted 7 July 2014)

We present a lecture demonstration that produces a visible, beating interference pattern that is the optical analog of demonstrations that produce audible, beating sound-wave interference. The setup is a compact, portable Mach-Zehnder interferometer made of optical components commonly found in laser physics laboratories. This apparatus may also be built and used in advanced laboratory courses to illustrate concepts in interferometry and laser light modulation. © 2014 American Association of Physics Teachers.

[<http://dx.doi.org/10.1119/1.4890502>]

When presenting demonstrations of the wave nature of light, instructors are often limited to static interference patterns formed by light waves diffracting through stationary slits or passing through an interferometer. Such static patterns arise from the relative phase differences of multiple wave paths. In contrast, to demonstrate the wave nature of sound, instructors most often present dynamic interference patterns using two tuning forks or sine-wave-driven speakers.¹ In such an experiment, the controlled relative frequency difference produces an audible, beating sound envelope. While optical analogs of such audio demonstrations exist,^{2–8} they seem to be rarely used, perhaps because of the perceived complexity and cost, and they usually rely on electronic detection of the interference. In this Note, we present a striking demonstration of dynamic light interference, visible by eye, which can be built simply, compactly, and relatively inexpensively by using (or borrowing) optical components commonly found in laser physics labs.

Figure 1 shows a schematic of the apparatus, which consists of a Mach-Zehnder interferometer⁹ modified to include two acousto-optic modulators (AOMs). Light from a He-Ne laser is split along two optical paths. Each path contains one AOM, which serves to shift the frequency of the light by an amount equal to the radio frequency (RF) of a sine-wave signal sent to the input of each AOM. This shift originates from

the light scattering off traveling pressure waves in a crystal, and resembles the Doppler shift of light scattering off a moving diffraction grating.⁸

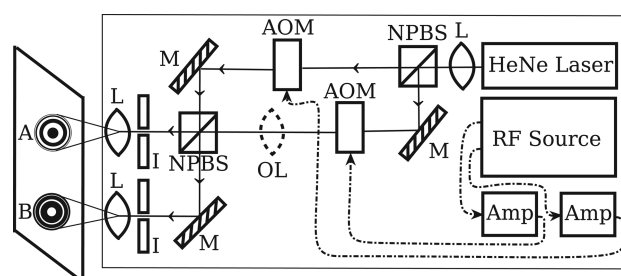


Fig. 1. Schematic diagram of the demonstration apparatus. A video showing the actual apparatus is available as an enhancement to Fig. 2. Laser light following the solid arrows produces two complementary interference patterns (A and B) that visibly beat at an optical frequency difference created by acousto-optic modulators (AOMs). A lens (L) directly after the laser output focuses light into the AOMs to improve diffraction efficiency, while an optional lens (OL) in one path alters the relative beam curvature, introducing circular fringes. Two more lenses expand the beams to enhance visibility of the interference pattern. Irises (I) block unwanted light produced by higher diffraction orders of the AOMs. Dashed arrows represent radio-frequency (RF) coaxial cables. Other components of the apparatus are amplifiers (Amp), mirrors (M), non-polarizing beam splitters (NPBS), and a two-channel RF frequency synthesizer (RF Source).

When the light beams from both paths are recombined, the resulting interference pattern beats at a rate equal to the difference between the optical frequencies of the paths, which is the same as the difference between the frequencies of the RF AOM signals. The beating of two superimposed beams of equal amplitudes E_0 oscillating at optical frequencies ω_1 and ω_2 can be written as

$$\begin{aligned} &|E_0 \cos(\omega_1 t) + E_0 \cos(\omega_2 t)|^2 \\ &= 2|E_0|^2 [1 + \cos(\omega_b t)] \cos^2(\bar{\omega} t), \end{aligned} \quad (1)$$

where $\omega_b = \omega_1 - \omega_2$ is the beat frequency and $\bar{\omega} = (\omega_1 + \omega_2)/2$ is the optical carrier frequency. The superposition is squared because our eyes are sensitive to intensity rather than amplitude. When the RF difference is 1 Hz, the interferometer output beats at 1 Hz, which is readily visible by eye. RF differences beyond about 20 Hz produce beats that are undetectable by eye, causing the interference pattern to wash out.

Figure 2 shows a time series of images of 2-Hz dynamic interference patterns produced by our apparatus. One benefit of the Mach-Zehnder configuration is that it produces two complementary interference patterns, labeled A and B, which can be viewed together. These patterns are the inverses of one another. The mechanism behind this inversion is not obvious. At first glance, the beam paths, each involving an equal number of reflections and transmissions, appear to be symmetric. However, a careful analysis reveals that a phase shift of either π or 0 radians occurs at each reflection, depending on whether light reflects from a “hard” surface ($n_f > n_i$) or a “soft” surface ($n_f < n_i$), resulting in the complementary patterns A and B.⁹

To enhance the visibility, we generated circular interference fringes using an optional lens (OL in Fig. 1) that creates different wavefront curvatures for the interfering beams.¹⁰ For equal RF AOM frequencies, the circular interference fringes are fixed. For unequal RF AOM frequencies, the circular interference fringes move radially inward or outward, depending on the sign of the frequency difference. For phase-continuous RF sources, such as the direct-digital-synthesis source we used, the circular fringes move continuously and do not jump, even while the frequency difference is changed.

There is flexibility in the type of laser used for this demonstration. In addition to the He-Ne laser, we successfully used both red and green laser pointers. Note that the frequency stability of the laser does not matter as long as the path-length difference between interferometer paths, typically 1 cm, is less than the coherence length of the laser, which

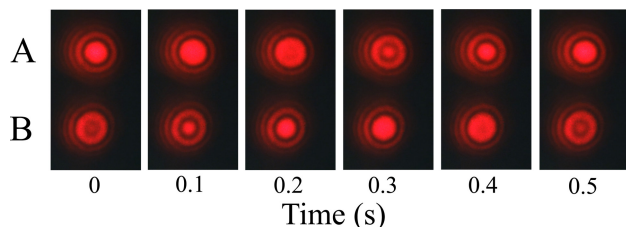


Fig. 2. (Color online) Images of beating interference patterns (A and B) created by a 2-Hz optical frequency difference. A video of these interference patterns is available as an online enhancement (enhanced online). [URL: <http://dx.doi.org/10.1119/1.4890502.1>]

usually ranges from 10 cm to hundreds of meters for He-Ne lasers. Inexpensive laser pointers with very short coherence lengths may require more precise interferometer alignment. The degree of linear polarization of the laser light, however, does affect the quality of the interference patterns. We found that placing a polarizer at the output of our HeNe laser helped to sharpen the contrast of the interference patterns.

The most expensive components required are the two AOMs and suitable RF frequency sources with Hz resolution, but these can often be found in (or borrowed from) modern undergraduate or research laboratories that use lasers or purchased inexpensively from surplus sources. For our apparatus, we used two identical 80-MHz Isomet model 1205C-2 AOMs (\$800 each), although AOMs with different operating frequencies can also be used. For example, our initial apparatus used one 80-MHz AOM operated near 95 MHz and another 210-MHz AOM operated near 190 MHz. To correct for the frequency difference, we passed light twice through the 80-MHz AOM. When acousto-optic modulators are not available, another option for shifting the frequency of laser light is to pass the beam through a transmission diffraction grating that is moving transverse to the beam. This technique produces a small Doppler shift $\Delta\nu = \pm mV/d$ in the m -th diffracted order of the beam, where V is the velocity of the grating and d the grating spacing.⁸

When using AOMs to provide the beat note, it is critical to drive them with a pair of RF sources capable of providing a stable Hz-level beat frequency. If independent RF sources are used, their stabilities must be better than $\sim 10^{-8}$ in order to ensure a steady ~ 1 Hz difference between AOMs driven at ~ 100 MHz. An easier and more economical solution is to use a two-channel frequency synthesizer with at least a 1-Hz resolution, which will guarantee phase coherence between the two AOM RF inputs. We used a Novatech model 409B/02 dual-channel RF synthesizer (\$895) with 1-W amplifiers [RF Bay MPA-10-40 (\$229) and Minicircuits ZHL-3A (\$229)]. Cheaper synthesizers, such as the Novatech DDS9m/02 (\$645), would be suitable as well.

In summary, we developed a portable, compact, and dynamic demonstration that uses optical self-heterodyning to allow students to directly observe, by eye, the wave nature of light, making use of an interferometer and acoustic-optic modulators to create a hertz-level frequency difference between lasers beams with absolute frequencies of hundreds of terahertz. We believe this will be a valuable addition to the repertoire of lecture demonstrations of the wave nature of light and additionally can serve as an educational platform for advanced students to learn the concepts of modulation and interferometry.

^aElectronic mail: mpm2153@columbia.edu

¹Derrick E. Boucher, “A visual and acoustic demonstration of beats and interference,” *Phys. Teach.* **37**, 177–178 (1999).

²Tomasz Kawalec and Dobrosława Bartoszek-Bober, “Two-laser interference visible to the naked eye,” *Eur. J. Phys.* **33**, 85–90 (2012).

³K. Razdan and D. A. Van Baak, “Demonstrating optical beat notes through heterodyne experiments,” *Am. J. Phys.* **70**, 1061–1067 (2002).

⁴Lorenzo Basano, Roberto Chittofrati, Stefano Crivello, Emanuele Piano, and Carlo Pontiggia, “Simple setup for detecting interference fringes produced by independent lasers,” *Am. J. Phys.* **65**, 996–1000 (1997).

⁵Lorenzo Basano and Pasquale Ottonello, “Interference fringes from stabilized diode lasers,” *Am. J. Phys.* **68**, 245–247 (2000).

⁶F. Louradour, F. Reynaud, B. Colombeau, and C. Froehly, “Interference fringes between two separate lasers,” *Am. J. Phys.* **61**, 242–245 (1993).

⁷S. F. Jacobs, "Optical heterodyne (coherent) detection," *Am. J. Phys.* **56**, 235–245 (1988).

⁸R. Corey, A. Schmidt, and P. Saulnier, "Using a moving diffraction grating to simulate the function of an acousto-optic modulator," *Am. J. Phys.* **64**, 614–617 (1996).

⁹K. P. Zetie, S. F. Adams, and R. M. Tocknel, "How does a Mach-Zehnder interferometer work?," *Phys. Educ.* **35**, 46–48 (2000).

¹⁰Paul Nachman, "Mach-Zehnder interferometer as an instructional tool," *Am. J. Phys.* **63**, 39–43 (1995).

Simple and inexpensive stereo vision system for 3D data acquisition

Samuel E. Mermall and John F. Lindner

Department of Physics, The College of Wooster, Wooster, Ohio 44691

(Received 3 June 2013; accepted 7 May 2014)

We describe a simple stereo-vision system for tracking motion in three dimensions using a single ordinary camera. A simple mirror system divides the camera's field of view into left and right stereo pairs. We calibrate the system by tracking a point on a spinning wheel and demonstrate its use by tracking the corner of a flapping flag. © 2014 American Association of Physics Teachers.

[<http://dx.doi.org/10.1119/1.4878560>]

I. INTRODUCTION

Recent techniques to track objects in instructional physics labs include LED sensors and finely-ruled mylar strips on air tracks,¹ a Nintendo *Wii* Remote (Wiimote) game controller,² and a Microsoft Xbox 360 video game Kinect sensor.³ In addition, video has long been used to study motion in undergraduate physics labs, including underdamped pendulums,⁴ rigid bodies and normal modes,⁵ and coupled oscillators.⁶ Automated 2D tracking systems exploit contrast⁷ and color.⁸ Commercial 3D tracking systems use dual infrared⁹ or visible light¹⁰ cameras.

This paper describes an inexpensive 3D tracking system that requires only a single off-the-shelf digital camera. A simple external mirror system divides the camera's field of view into left and right stereo pairs. Software tracks objects in both fields and simple projection equations reconstruct 3D trajectories. The relevant theory is discussed in Sec. II and the apparatus and its calibration are described in Sec. III. An example experiment is the focus of Sec. IV and the limitations and extensions of the technique are discussed in Sec. V.

II. TRAJECTORY RECONSTRUCTION

Epipolar geometry^{11,12} describes the relationship between two cameras photographing the same scene from different points of view. For simplicity, the cameras are modeled as pinholes with a focal length $f < 0$ and a baseline separation $b > 0$, as shown in Fig. 1. The optical axes of the left and right cameras, L and R , are assumed to be parallel. The cameras capture 2D $\{x, y\}$ images of the 3D $\{X, Y, Z\}$ world. Using the similar right triangles shown in Fig. 1, where $X < 0$, it is clear that $-x_L/f = -X/Z$ and $-x_R/f = (-X + b)/Z$. The difference $(x_L - x_R)/f = b/Z$ can be used to determine the depth $Z = bf/(x_L - x_R)$. The X and Y coordinates can be determined from the x and y positions recorded by the left camera: $X = x_L Z/f$ and $Y = y_L Z/f$. The 3D $\{X, Y, Z\}$ coordinates are thus

$$X = b \frac{x_L}{x_L - x_R}, \quad (1a)$$

$$Y = b \frac{y_L}{x_L - x_R}, \quad (1b)$$

$$Z = b \frac{f}{x_L - x_R}. \quad (1c)$$

If the left camera is rotated through a small angle $0 < \theta \ll 1$ about the Y -axis, clockwise in Fig. 1, the optical axes intersect at a *fixation point* near $\{b, 0, b/\theta\}$ and shift the left projection slightly, from x_L to $x_L - f\theta$. The 3D coordinates are now

$$X' \approx b \frac{x_L - f\theta}{x_L - x_R - f\theta}, \quad (2a)$$

$$Y' \approx b \frac{y_L}{x_L - x_R - f\theta}, \quad (2b)$$

$$Z' \approx b \frac{f}{x_L - x_R - f\theta}. \quad (2c)$$

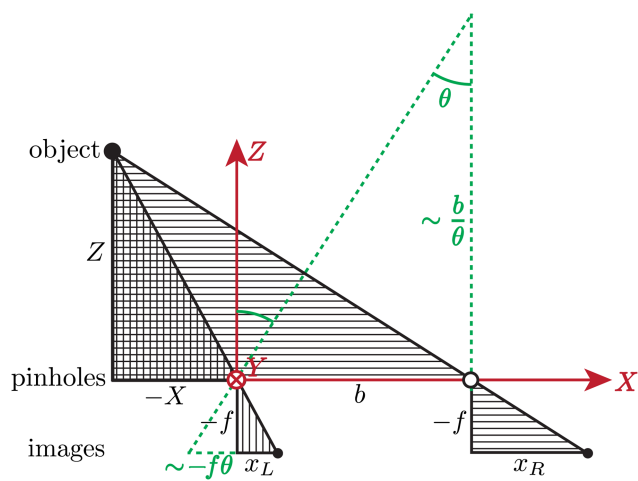


Fig. 1. Similar right triangles in the XZ -plane of the stereo geometry, with pinhole approximations for the camera lenses. The distances $-X > 0$ and $-f > 0$ and the tilt angle θ are exaggerated.